C66

Inhibition of either protein tyrosine kinases or phosphatases strongly inhibits the secretion but not the synthesis of serum albumin by rat hepatocytes

J.D. Judah, R.J. Webb, A. Knezevic and G.M.H. Thomas

Department of Physiology, University College London, Rockefeller Building, 21 University Street, London WC1E 6JJ, UK

Serum albumin is the major soluble protein constituent of blood serum. The biosynthsis and secretion of albumin is, in terms of mass, the principal endocrine protein secretory event in the bodies of almost all animals. To date there is no evidence to suggest that either the processes of synthesis or secretion are regulated other than by gene transcription.

Male Sprague-Dawley rats (approximately 250 g) were anaesthetised with halothane and then killed humanely (in accordance with both local and national guidelines). After cannulation of the hepatic portal vein the liver was perfused with Ringer solution containing 2 mM EGTA. The tissue was cut into small pieces passed though a sieve and the hepatocytes recovered on a discontinuous Percol gradient. Live cells (> 95 % viable by dye exclusion) were cultured overnight in Williams E medium supplemented with insulin and serum in collagen-coated plastic dishes.

For the experiments albumin was radiolabelled with methionine using a 'pulse-chase' protocol. Secretion of the newly synthesised albumin was allowed to proceed for 30 min at 37 °C. Albumin and its immediate metabolic precursor proalbumin, were recovered for the supernatant and the cells by immuno-precipitation and quantitated by phosphoimaging. All data were analysed with paired two-tailed t tests, allowing for unequal variance, and are shown with S.E.M. Data are expressed as the percentage of total newly synthesised albumin secreted in 30 min.

Firstly, we found that normally 51 ± 2 % (n = 25) of the newly synthesised albumin was secreted. Secondly, the treatment of the cells with several drugs caused severe disruption of albumin secretion. The inhibitors of Golgi body function, Brefeldin A (10 μg ml^{-1}) and monensin (3 μg ml^{-1}), were used as positive controls and showed very strong inhibition of albumin secretion (reduced to 5 ± 4 and 7 ± 5 %, respectively, n = 5 each). This is as expected. In addition, broad-spectrum inhibitors of protein tyrosine kinases (genistein, 100 μM) and phosphatases (vanadium peroxide, 100 μM) both caused strong inhibition (reduced to 21 ± 8 and 20 ± 5 %, respectively, n = 4 each). Lastly, microscopic examination of the Golgi indicated that the same drugs caused clearly observable changes in the subcellular distribution of Golgi-resident proteins.

We conclude that at least one protein tyrosine kinase and phosphatase play significant roles in the secretion of albumin from rat hepatocytes.

All procedures accord with current UK legislation.

C67

Ca^{2+} signalling and gap junctional communication in the neural retina and retinal pigment epithelium of the embryonic chick eye

R. Pearson*, M. Catsicas*, D. Becker† and P. Mobbs*

*Departments of *Physiology and †Anatomy and Developmental Biology, University College London, Gower Street, London WC1E 6BT, UK*

In the neural retina (NR), the proliferation of progenitor cells (PCs) and cell differentiation are tightly regulated to ensure the right numbers of each retinal cell type are present in the adult retina. Studies of albino animals (Ilia & Jefferey, 2000) suggest that the retinal pigment epithelium (RPE) may play an important role in the regulation of these processes. In order to better understand the physiological relationship between the NR and the RPE we have examined the role of gap junctions and purinergic receptors in Ca^{2+} signalling in these two tissues.

Retinas (NR and RPE) from embryonic day 4 (E4) to E6 chicks killed by decapitation were dissected in Krebs solution gassed with 95 % O_2 and 5 % CO_2. Using either patch pipettes or sharp microelectrodes, single RPE cells were filled, in control solution or in the presence of the gap junction blocker carbenoxolone, with FITC-Dextran (3000 MW) and Neurobiotin (NB, 256 MW), a combination which marks the injected cell with FITC and any cells coupled to it with NB. Retinas were fixed in 4 % formaldehyde and processed to reveal the NB with Cy3-avidin. Dye-filled cells were imaged on a confocal microscope. Some retinas were subsequently immunostained using an antibody to neuron-specific β-tubulin (TUJ-1) to identify differentiating neurons and re-imaged. Our results show that at E4 RPE cells are coupled via gap junctions both to one another (n = 59 dye fills) and to PCs in the NR (n = 30 dye fills). Coupling to the NR disappears by E6.

Changes in $[Ca^{2+}]_i$ in the RPE and NR and the progress of mitosis were simultaneously monitored on the confocal microscope at 36 °C. This was done by first loading retinas with either Oregon Green-BAPTA-AM or fluo-4 AM (10 μM for 1 h) and then, during the imaging process, superfusing them with the vital chromatin dye Hoechst 33342 (2 μM). These experiments show that periodic spontaneous Ca^{2+} signals propagate via gap junctions in both RPE (n = 6 retinae) and NR (n = 8 retinae) and that, albeit rarely, Ca^{2+} signals pass between the two tissues. Ca^{2+} transients propagated as waves that invaded many cells in the RPE while in the NR Ca^{2+} activity was more spatially restricted. The presence of the RPE and purinergic agonists and antagonists had profound effects on the rate of mitosis in the NR that may be mediated by ATP release from the RPE and purinergic receptors present on dividing cells in the NR. Further experiments are required to investigate the role of $[Ca^{2+}]_i$ transients and purinergic signalling in the NR and RPE in the regulation of mitosis in the developing retina.

Ilia M & Jeffery G (2000). *J Comp Neurol* **420**, 437–444.

This work was supported by the BBSRC, MRC, Wellcome Trust and the Royal Society.

All procedures accord with current UK legislation.

C68

PKCβ2-dependent phosphorylation of core 2 GlcNAc-T promotes leucocyte–endothelial cell adhesion: a mechanism underlying capillary occlusion in diabetic retinopathy

Rakesh Chibber*, Bahaedin M. Ben-Mahmud*, Giovanni E. Mann*, Jin J. Zhang† and Eva M. Kohner‡

*Centre for Cardiovascular Biology & Medicine, GKT School of Biomedical Sciences, King's College London, Guy's Campus, London SE1 1UL, †GKT Department of Ophthalmology, The Rayne Institute, St Thomas' Hospital, London and ‡Department of Endocrinology, Diabetes & Internal Medicine, St Thomas' Hospital, Lambeth Wing, Lambeth Palace Road, London SE1 7EH, UK

Increased leukocyte–endothelial cell adhesion is a key early event in the development of retinopathy and atherogenesis in diabetic patients. We recently reported that raised activity of glycosylating enzyme β-1,6-acetylglucosaminyltransferase (core 2 GlcNAc-T) is responsible for increased leukocyte-endothelial cell adhesion and capillary occlusion in retinopathy. Here we demonstrate that elevated glucose and diabetic serum increase the activity of core 2 GlcNAc-T (2040 ± 445 (15 mM glucose, $n = 5$) *vs.* 182.7 ± 65.5 (5.8 mM glucose, $n = 5$); $P = 0.0033$; 2035 ± 411 (diabetic serum, $n = 25$) *vs.* 196 ± 35 (control serum, $n = 19$), $P = 0.0002$) and adhesion of human leukocytes to retinal capillary endothelial cells (8.76 ± 0.5 (15 mM glucose, $n = 18$) *vs.* 3.7 ± 0.35 (5.8mM glucose, $n = 18$), $P = 0.0001$; 3.7 ± 0.48 (diabetic serum, $n = 21$) *vs.* 0.62 ± 0.09 (control serum, $n = 15$), $P = 0.0001$) through diabetes activated serine/threonine protein kinase C b2 (PKCb2)-dependent phosphorylation. This regulatory mechanism, involving phosphorylation of core 2 GlcNAc-T, is also present in polymorphonuclear leukocytes (PMNs) isolated from Type 1 and Type 2 diabetic patients. Inhibition of PKCb2 activation with the specific inhibitor, LY379196, attenuated serine phosphorylation of core 2 GlcNAc-T and prevented increased leukocyte-endothelial cell adhesion. Raised activity of core 2 GlcNAc-T was associated with a 3-fold increase in O-linked glycosylation of P-selectin glycoprotein ligand-1 (PSGL-1) on the surface of leukocytes of diabetic patients compared to age-matched controls. PKCb2-dependent phosphorylation of core 2 GlcNAc-T may thus represent a novel regulatory mechanism for activation of this key enzyme in mediating increased leukocyte-endothelial cell adhesion and capillary occlusion in diabetic retinopathy.

Bevilacqua MP *et al.* (1994). *Ann Rev Med* **45**, 361–378.

Chibber R *et al.* (2000). *Diabetes* **49**, 1724–1730.

Joussen AM *et al.* (2001). *Am J Pathol* **158**, 147–152.

Koya D *et al.* (1998). *Diabetes* **47**, 859–866.

Miyamoto K *et al.* (1999). *Proc Natl Acad Sci USA* **96**, 10836–10841.

We thank Dr Allassandro Datti (Genetics Institute, Canada) for supplying the core 2 GlcNAc-T antibody. We also thank Dr Kumar (Genetics Institute, Canada), Professor Alan Fields and Dr Nicole Murphy (Sealey Center for Cancer Research, Galvaston, Texas, USA) for the PKCβ2 cDNA plasmid for transfection experiments, and Mr John Schilling (Eye Unit, St Thomas' Hospital) for blood samples from diabetic patients. This study was supported by the Juvenile Diabetes Foundation International (JDFI).

C69

P2X receptor blockade by the pH indicator dye, Phenol Red

B.F. King*‡, M. Liu*, S.G. Brown*, G. Knight*, A. Townsend-Nicholson*†, P.M. Dunn*, S.S. Wildman‡, V.M. Jackson§, T.C. Cunnane§, J. Pfister‖, F. Padilla‖, A.P. Ford‖ and G. Burnstock*

*Anatomy & Developmental Biology, †Biochemistry & Molecular Biology and ‡Physiology, University College London, §Pharmacology, Oxford and ‖Roche Bioscience, Palo Alto, California, USA

Phenol Red (phenolsulphophthalein sodium salt, 376.4 amu; Aldrich) is a water-soluble pH indicator dye (pH 6.2–8.2, yellow-to-red colour transition), commonly found in culture media (e.g. Dulbecco's modified Eagle's medium (DMEM); at 15 mg l^{-1} (40 μM)). Here, we report that this compound also inhibits ATP-evoked ion currents at rat P2X (rP2X) receptors heterologously expressed in defolliculated *Xenopus laevis* oocytes.

Under voltage-clamp conditions (V_h, −30 mV), ATP (applied at its EC_{70} value) evoked inward ion currents at homomeric P2X receptors, which were inhibited by commercially available Phenol Red with the following potency order (mean pIC_{50}, $n = 4$): $rP2X_1$ (5.48) > $rP2X_3$ (4.60) > $rP2X_2$ (4.19) > $rP2X_4$ (< 4.00) – where inhibition was reversed following washout. Purified Phenol Red also inhibited P2X receptors without altering mean pIC_{50} values ($rP2X_1$ (5.41) and $rP2X_3$ (4.67); $n = 4$). For concentration/ response (C/R) curves to ATP and α,β-meATP, Phenol Red (1–100 μM) inhibited agonist responses at $rP2X_1$ and $rP2X_3$ receptors in a non-surmountable manner.

Under whole-cell patch-clamp conditions (V_h, −60 mV), $P2X_3$-like ATP responses in isolated rat DRG neurons were inhibited by Phenol Red (30 μM). At rat vas deferens, $P2X_1$-like contractions evoked by either purinergic neurotransmission or exogenous ATP were weakly inhibited by Phenol Red (100 μM). Closer inspection of C/R curves for exogenous ATP revealed two phases – where the initial phase was inhibited by Phenol Red (1, 3 and 10 μM). α,β-MeATP responses in rat vas deferens were inhibited in a surmountable manner by Phenol Red (10, 30 and 100 μM). Electrically evoked purinergic EJPs in mouse vas deferens were not inhibited by Phenol Red (300 μM). Animals were killed by cervical dislocation.

Our results show that Phenol Red (or residual impurity therein) blocks recombinant $rP2X_1$ and $rP2X_3$ subtypes in a non-surmountable, yet reversible, manner. This antagonist is also effective at native $P2X_3$-like receptors in rat tissue. However, Phenol Red was largely ineffective at $P2X_1$-like electrical (mouse) and mechanical (rat) responses in vas deferens, although $P2X_1$ plays a critical role in this tissue since purinergic responses disappear in $P2X_1$ gene-deleted mice (Mulryan *et al.* 2000). Our results suggest that the $P2X_1$ subunit mediates purinergic signalling in the vas deferens through the formation of a heteromeric purinoceptor of unknown molecular composition and that homomeric $P2X_1$ receptors do not predominate in this tissue.

Mulryan K *et al.* (2000). *Nature* **403**, 86–89.

All procedures accord with current UK legislation.

C72

A P_{O_2} window for smooth muscle cADPR accumulation and constriction by hypoxia in rabbit pulmonary artery smooth muscle

Michelle Dipp†, Justyn M. Thomas‡, Antony Galione‡ and A. Mark Evans*

**School of Biology, Bute Building, University of St Andrews, St Andrews, Fife KY16 9TS, †University Laboratory of Physiology, Parks Road, Oxford OX1 3PT and ‡University Department of Pharmacology, Mansfield Road, Oxford OX1 3QT, UK*

Hypoxic pulmonary vasoconstriction (HPV) is unique to pulmonary arteries, and aids ventilation/perfusion matching. However, in diseases like emphysema HPV can promote hypoxic pulmonary hypertension. Our previous investigations have demonstrated that the calcium mobilising second messenger cyclic adenosine diphosphate ribose (cADPR) is an important mediator of HPV (Wilson *et al.* 2001; Dipp & Evans, 2001). We describe here the relationship between the degree of hypoxia, cADPR levels and HPV in isolated rabbit pulmonary arteries. (Male New Zealand White rabbits were killed humanely by cervical dislocation.) In intact pulmonary arteries HPV was reproducible when stepping from a gas mixture containing 20 % O_2 to one containing 2 % O_2. Under these conditions a typical biphasic constriction was observed: an initial transient constriction followed by a slow tonic constriction. When we stepped from 20 % O_2 to 0 % O_2, however, the transient constriction increased in magnitude by approximately 10 % ($n = 4$). Surprisingly, however, phase 2 of HPV was abolished (Fig. 1).

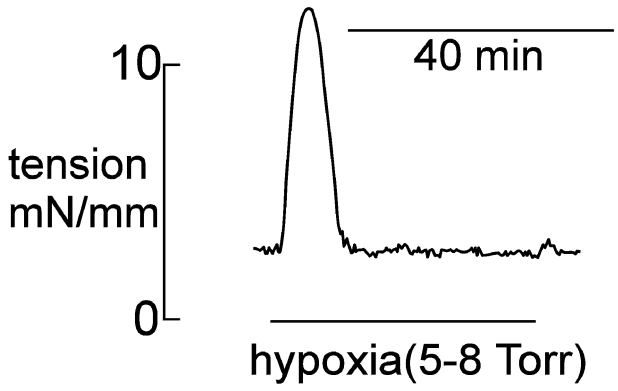

Figure 1.

In arteries without endothelium, stepping from 20 % O_2 to 2 % O_2 induced an initial transient constriction followed by a maintained cADPR-dependent plateau constriction. Once again, stepping from 20 % O_2 to 0 % O_2 augmented the initial transient constriction whilst abolishing the maintained plateau constriction ($n = 4$). The relationship between P_{O_2} and cADPR accumulation in the smooth muscle was also bell-shaped, consistent with the view that the plateau constriction by hypoxia is mediated by cADPR-dependent SR Ca^{2+} release. Thus hypoxia (16–21 Torr) increased cADPR content from 1.8 ± 0.04 pmol (mg protein)$^{-1}$ (mean ± S.E.M.) to 19.7 ± 1.1 pmol (mg protein)$^{-1}$ ($n = 3$), which returned to 1.91 ± 0.06 pmol (mg protein)$^{-1}$ in near-anoxic conditions (5–8 Torr; $n = 3$). We conclude that there is a P_{O_2} window within which cADPR accumulation in pulmonary artery smooth muscle and maintained HPV may be induced by hypoxia. Our previous findings suggested that an increase in β-NADH levels by hypoxia may result in inhibition of cADPR hydrolase activity and thereby promote, in part, cADPR accumulation (Wilson *et al.* 2001). However, we now propose that anoxia promotes a further reduction in β-NAD^+ availability, leading to a situation where the supply of substrate (β-NAD^+) for cADPR synthesis becomes rate limiting. As a consequence, increased β-NADH formation under anoxic conditions will result in a fall in cADPR accumulation and reversal/attenuation of HPV.

Dipp M & Evans AM (2001). *Circ Res* **89**, 77–83.
Wilson HL *et al.* (2001). *J Biol Chem* **276**, 11180–11188.

All procedures accord with current UK legislation.

C73

Inositol 1,4,5-trisphosphate receptors are required for capacitative calcium entry

Claire M. Peppiatt, Martin D. Bootman, Michael J. Berridge and H. Llewelyn Roderick

The Babraham Institute, Babraham, Cambridge CB2 4AT, UK

Capacitative calcium entry (CCE) is the process by which depletion of intracellular calcium stores leads to the activation of calcium influx at the plasma membrane. It has been proposed that inositol 1,4,5-trisphosphate ($InsP_3$) receptors ($InsP_3Rs$) sense the reduction of calcium within calcium stores and control the opening of channels at the plasma membrane via direct physical interaction. Likely candidates for the CCE channels are members of the transient receptor potential (TRPC) family. Using heterologous expression of the proposed interacting domains of TRP and $InsP_3Rs$, and manipulation of intracellular $InsP_3$ levels, we examined the necessity for $InsP_3Rs$ in the activation of CCE.

Intracellular calcium levels were monitored in HEK-293 cells using fura-2 (30 min loading with acetoxymethyl ester followed by a 30 min de-esterification period) at room temperature. CCE was activated by depletion of intracellular stores with thapsigargin (1 μM) in calcium-free medium. The peak calcium rise following re-addition of calcium to the extracellular medium was taken as the index of CCE activation. Heterologous expression of eGFP-tagged proteins was achieved using standard transfection procedures. Data are presented as means ± S.E.M. Statistical significance was calculated using Student's unpaired *t* test. For the heterologous expression experiments, control and test cells were imaged in the same fields of view, with the transfected cells identified by eGFP fluorescence.

Expression of the domain of TRP3 (amino acids 742 to 797) proposed to interact with $InsP_3Rs$ decreased the peak CCE signal from 477 ± 34 to 307 ± 23 nM ($n = 20$). In contrast, the domain of $InsP_3R3$ (amino acids 638 to 710) that has been suggested to interact with TRP3 did not alter peak CCE levels. Manipulation of intracellular $InsP_3$ levels was achieved using expression of type 1 $InsP_3$ 5′-phosphatase or a ligand binding 'sponge' domain of the $InsP_3R$. Both moieties completely inhibited calcium release via the $InsP_3$-linked agonist ATP (100 μM), without changing the size of the intracellular calcium store. 5′-Phosphatase expression reduced CCE from 463 ± 22 nM ($n = 47$ cells) to 369 ± 23 nM ($n = 25$ cells) ($P < 0.05$). Similarly, the $InsP_3$ sponge decreased CCE from 432 ± 38 nM ($n = 15$ cells) to 301 ± 27 nM ($n = 18$ cells) ($P < 0.05$). $InsP_3$ production was inhibited using the phospholipase C antagonist U73122 (10 μM), which completely blocked ATP-induced calcium mobilisation. Treatment with U73122 resulted in a decreased peak CCE signal from 989 ± 116 nM ($n = 25$ cells) to 210 ± 16 nM ($n = 23$ cells) ($P < 0.05$).

These data are consistent with a requirement for both $InsP_3$ and $InsP_3Rs$ in the activation of CCE.

Rosado JA *et al.* (2002). *J Biol Chem* (DOI: 10.1074/jbc.M207320200).
Rosado JA *et al.* (2000). *J Biol Chem* **275**, 7527–7533.
Rosado JA & Sage SO (2000). *Biochem* **350**, 631–635.

This work was supported by vacation studentships from the Nuffield Foundation (A.G.S.H.) and The Wellcome Trust (M.T.H.).

C74

A role for Trp1 and lipid raft domains in store-mediated Ca^{2+} entry in human platelets

Alan G.S. Harper, Matthew T. Harper, Sharon L. Brownlow and Stewart O. Sage

Department of Physiology, University of Cambridge, Cambridge CB2 3EG, UK

We have presented evidence that in human platelets store-mediated Ca^{2+} entry (SMCE) involves secretion-like coupling between the human homologue of the *Drosophila* transient receptor potential channel, hTrp1, and the type II inositol 1,4,5-trisphosphate receptor (Rosado *et al.* 2000; Rosado & Sage, 2000; Rosado *et al.* 2002). In other cells Trp1 has been reported to be associated with cholesterol-rich lipid raft domains (LRDs) in the plasma membrane, which form the basis for its assembly into signalling complexes (e.g. Lockwich *et al.* 2000). LRDs have recently been demonstrated in platelets (Gousset *et al.* 2002) and here we have investigated whether hTrp1 is functionally associated with these domains.

Blood was drawn from healthy, drug-free volunteers with local ethical committee approval. Platelets were prepared, fluorescence measured and hTrp1 detected as previously described (Rosado & Sage, 2000). Platelet membranes were prepared as described by Gousset *et al.* (2002). Thapsigargin (TG)-induced Ca^{2+} entry was estimated as the integral of the rise in $[Ca^{2+}]_i$ for 2.5 min after addition of Ca^{2+}. Thrombin-evoked Ca^{2+} influx was estimated as the integral of the rise in $[Ca^{2+}]_i$ above basal for 2 min after addition of thrombin, corrected by subtraction of the response in the absence of external Ca^{2+} (1.2 mM EGTA added).

Trp1 was found to be associated with platelet membranes and remained associated with membranes to a large degree after detergent (1% Triton X-100) treatment for 30 min at 37°C, although Triton released some hTrp1 into the solubilizate. After cholesterol depletion of the membrane by treatment with methyl-β-cyclodextrin (MBCD; 10 mM for 30 min at 37°C), detergent treatment decreased the amount of hTrp1 associated with the membrane fraction and increased that in the solubilizate.

Cholesterol depletion using MBCD (10 mM) reduced Ca^{2+} release evoked by thrombin (1 U ml^{-1}) to 70.3 ± 3.8% of control (mean ± S.E.M.; $n = 13$). Under the same conditions the inhibition of Ca^{2+} entry was significantly greater ($P < 0.001$; Student's unpaired t test), being reduced to 48.2 ± 4.5% of control (mean ± S.E.M.; $n = 13$). To investigate the effect of cholesterol depletion on SMCE alone, cells were treated with TG (200 nM) for 3 min in the presence of 200 μM EGTA to deplete the Ca^{2+} stores. SMCE was then assessed by raising external $[Ca^{2+}]$ to 300 μM. Cholesterol depletion using MBCD inhibited SMCE in a concentration-dependent manner, reducing it to 38.1 ± 4.1% of control (mean ± S.E.M.; $n = 13$) after treatment with 10 mM MBCD. TG-evoked Ca^{2+} release was unaffected by MBCD.

These results suggest that hTrp1 is present in LRDs in human platelets and that these domains are involved in SMCE in these cells.

Gousett K *et al.* (2002). *J Cell Physiol* **190**, 117–128.
Lockwich TP *et al.* (2000). *J Biol Chem* **275**, 11934–11942.

C75

Agonist-induced phosphatidylinositol-4,5-bisphosphate (PIP_2) hydrolysis and M-current inhibition in sympathetic neurons: effects of the neuronal calcium-sensor protein NCS1

J.S. Winks and S.J. Marsh

Department of Pharmacology, University College London, London, UK

$G_{q/11}$ G protein-coupled receptors stimulate PIP_2 hydrolysis. This can be monitored at the single-cell level by translocation of the green fluorescent protein-tagged Pleckstrin Homology domain of phospholipase C δ (GFP-PLCδ-PH; Stauffer *et al.* 1998). We have used this method to monitor PIP_2 hydrolysis in dissociated sympathetic neurons in parallel with voltage-clamp measurements of agonist-induced M-current (I_M) inhibition.

GFP-PLCδ-PH was expressed in superior cervical ganglion neurons (SCGs) from 17-day-old rats (killed humanely: Home Office Schedule 1 procedure) via intranuclear injection of a cDNA plasmid. One day after injection, whole-cell M-currents were recorded using perforated-patch electrodes, and localisation of GFP-PLCδ-PH monitored via fluorescence microscopy. At rest, GFP-PLCδPH was located preferentially at the plasma membrane. Application of either the muscarinic acetylcholine receptor agonist oxotremorine M (oxo M; 10 μM) or bradykinin (BK; 100 nM) induced reversible translocation of GFP-PLCδ-PH from membrane to cytosol, in parallel with I_M inhibition. The PI3/4-kinase inhibitor wortmannin (20 μM) prolonged reversal of both.

Over-expression of the neuronal calcium sensor protein 1 (NCS-1; Burgoyne & Weiss, 2001) reduced BK-induced inhibition of I_M 2 days after injection (100 nM BK) from 43.0 ± 9.0% (mean ± S.E.M., $n = 5$) in control cells to 14.1 ± 4.4% ($n = 6$). The muscarinic inhibition of I_M (10 μM oxo M) was unaltered (66.0 ± 9.1% ($n = 5$) − control, and 57.2 ± 7.8% ($n = 6$) − NCS-1).

Oxo M- and BK-induced translocation of GFP-PLCδ-PH were measured as a rise in cytosolic fluorescence intensity (CFI). In the control group, the rises in CFI induced by both agonists were almost equal, the average BK-induced rise being 98% of that induced by oxo M. The amplitude of the oxo M-induced rise in CFI was unchanged by NCS-1 overexpression. However, the BK-induced rise was significantly reduced.

These data extend recent electrophysiological observations relating PIP_2 turnover with I_M inhibition (Suh & Hille, 2002). Our results also indicate that NCS-1 reduces the sensitivity of I_M inhibition to BK by reducing the loss of PIP_2 from the membrane during agonist stimulation. We suggest that this is via an enhancement of PIP_2 synthesis, through increased PI4-kinase activity (Koizumi *et al.* 2002).

Burgoyne RD & Weiss JL (2001). *Biochem J* **353**, 1–12.
Koizumi S *et al.* (2002). *J Biol Chem* **277**, 30315–30324.
Stauffer TP *et al.* (1998). *Curr Biol* **8**, 343–346.
Suh B & Hille B (2002). *Neuron* **35**, 507–520.

This work was supported by The Wellcome Trust and the Medical Research Council. We thank Dr J.L.Weiss (University of Sheffield) for the NCS-1 cDNA and Dr T. Meyer (Duke University) for the GFP-PLCδ-PH.

All procedures accord with current UK legislation.

C76

The gain of calcium-induced calcium release is set by the holding potential

H. Griffiths and K.T. MacLeod

Department of Cardiac Medicine, NHLI, Imperial College, Dovehouse Street, London SW3 6LY, UK

We have shown previously that the concentrations of L-type Ca^{2+} channel blockers used during development of the voltage-sensitive release mechanism (VSRM) hypothesis, failed to exclude completely transmembrane Ca^{2+} entry (Griffiths & MacLeod, 2001). We formulated the hypothesis that calcium-induced calcium release (CICR) operated with increased gain under conditions necessary for the VSRM. An experiment was designed to evaluate the effect of holding potential on the gain of excitation–contraction coupling.

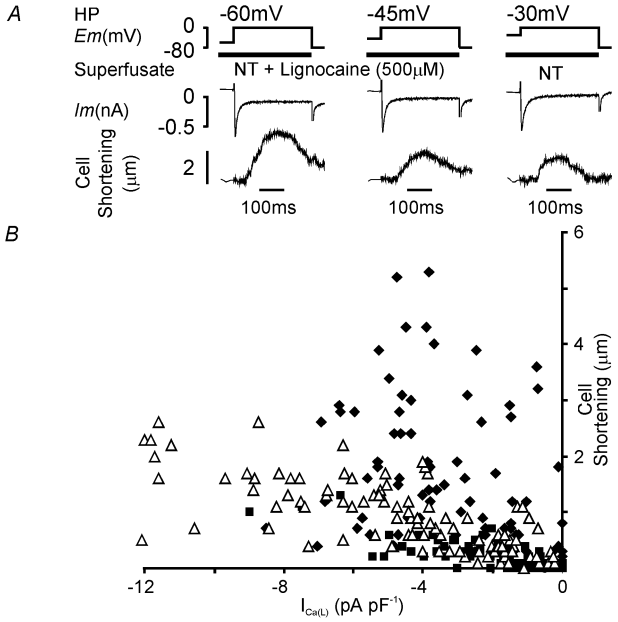

Figure 1. *A*, during superfusion with normal Tyrode solution (NT) for depolarisation from holding potential (HP) −30 mV and with NT + lignocaine for depolarisation from HP −60 and −45 mV, $I_{Ca(L)}$ amplitude was comparable for all holding potentials. Cell shortening amplitude diminished progressively with more depolarised holding potentials. *B*, cell shortening amplitude as a function of $I_{Ca(L)}$ density during depolarisation to 0 mV from HP −60 mV (◆), −45 mV (△) and −30 mV (■), $n = 27$. The three populations of points were significantly different ($P < 0.0001$, $n = 27$).

Rabbits were killed humanely by intravenous injection of 300 mg pentobarbitone. Enzymatically dissociated ventricular myocytes were held under single electrode voltage clamp at 37 °C. Intracellular dialysis was minimised with the use of high resistance microelectrodes. Cell shortening was recorded with a video edge-detection system. Gain was defined as cell shortening per unit $I_{Ca(L)}$ amplitude during depolarisation to 0 mV. Na^+ channels were blocked with lignocaine (500 μM) and $I_{Ca(L)}$ was partially blocked with lignocaine (500 μM) and $CdCl_2$ in a range of concentrations (0–10 μM). Sarcoplasmic reticulum (SR) Ca^{2+} content was kept constant by trains of depolarising steps. SR Ca^{2+} content was measured by integration of the inward current activated by rapid application of caffeine (10 mM).

Cell shortening was elicited by depolarisation from holding potentials of −60, −45 and −30 mV to an activating potential of 0 mV. Cell shortening was plotted as a function of $I_{Ca(L)}$ for each holding potential and the three relationships tested for independence by analysis of co-variance (ANCOVA). Gain was a function of the holding potential from which the cell was depolarised (Fig. 1). This has not previously been demonstrated.

SR Ca^{2+} content was also dependent on holding potential and was higher as holding potential became more negative (Fig. 2). The increased gain of CICR at negative holding potentials may be the result of increased SR Ca^{2+} content.

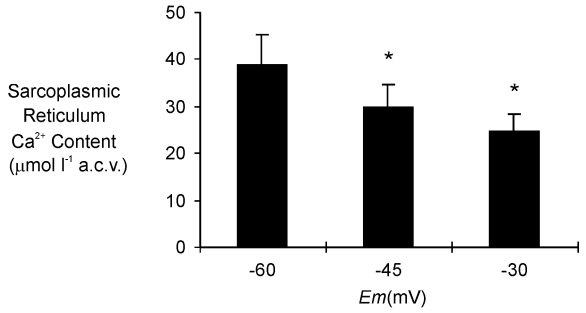

Figure 2. Means ± S.E.M. shown; a.c.v., accessible cell volume; *$P < 0.05$ by paired t test, $n = 17$.

Griffiths H & MacLeod KT (2001). *Circulation* **104**, II-194.

All procedures accord with current UK legislation.

C77

Nuclear envelopes from cerebellar Purkinje and granule cells express different types of ionic channels

Sergey M. Marchenko

Bogomoletz Institute of Physiology, 4 Bogomoletz Street, Kiev 01024, Ukraine

The nuclear envelope is a part of the endoplasmic reticulum big enough to be studied with the patch-clamp technique. A variety of ion channels in the outer nuclear membrane have been reported in different animal and plant cells (Mazzanti *et al.* 2001). Here I report for the first time the recording of ionic channels from the nuclear membranes of neurons. This is also the first report of patch-clamp recording from the inner nuclear membrane.

Thin cerebellar slices were prepared from the brains of 21- to 28-day-old male Wistar rats, killed by cervical dislocation. Cell bodies of the Purkinje and granule cells were collected from the slices and gently homogenised in solution containing (mM): 100 potassium gluconate, 50 KCl, 5 $MgCl_2$, 0.05 $CaCl_2$, 0.5 EGTA and 10 Hepes; pH 7.3. The homogenate was placed into a working chamber. The nuclei were allowed to attach to the glass bottom of the chamber and then washed from debris with the same solution, but without $MgCl_2$ and EGTA. Single ion channels were recorded from both nucleus-attached and excised patches of the outer and inner nuclear membranes with the patch-clamp technique. The patch electrode was filled with

solution containing (mM): 150 KCl, 0.05 $CaCl_2$ and 10 Hepes; pH 7.3. Experiments were conducted at room temperature (19–22 °C).

Ionic channels were detected in the nuclear membranes of both Purkinje and granule cells. The major channel (21 out of 29 patches) found in the nuclear membranes of Purkinje neurons was a cation-selective channel with the slope conductance of 198 ± 7 pS ($n = 21$ patches). This channel was especially abundant in the inner nuclear membrane of Purkinje cells where each patch contained ⩾ 2 channels. In contrast, the most common channel of the nuclear membranes of granule cells was the anion-selective channel. The anion channel had multiple conductance states with the slope conductance of the most common substate being 46 ± 5 pS ($n = 18$ patches). The nuclear membranes of granule neurones also contained a cationic channel with the slope conductance of 53 ± 4 pS ($n = 5$ patches).

These data suggest that different types of neurons express different classes of nuclear ion channels. The exact physiological role of nuclear channels is unknown. The nuclear envelope is a Ca^{2+} store, which implies large ion currents through the nuclear membranes. It is reasonable to suggest that nuclear channels are involved in the ionic homeostasis in the organelle. The expression of distinct types of ion channels in the nuclei of Purkinje and granule cells suggests different mechanisms of ionic homeostasis regulation in the nuclei of different neurons.

Mazzanti M *et al.* (2001). *Physiol Rev* **81**, 1–19.

This work was supported by the Wellcome Trust. I am grateful to R.C. Thomas for his department's hospitality in Cambridge and for help with supplies.

All procedures accord with current UK legislation.

PC30

Ryanodine receptor Ca^{2+} release during diastolic depolarization in cardiac pacemaker cells is independent of the depolarization

Tatiana M. Vinogradova and Edward G. Lakatta

Gerontology Research Center, National Institute on Aging, NIH, Baltimore, MD, USA

Studies employing confocal Ca^{2+} imaging have unequivocally implicated intracellular Ca^{2+} release as a modulator of beating rate of cardiac pacemaker cells (Rigg & Terrar, 1996; Huser *et al.* 2000; Bogdanov *et al.* 2001). In sino-atrial nodal cell (SANC), local subsarcolemmal ryanodine receptor (RyR) Ca^{2+} release during the diastolic depolarization (CRDD) activates the electrogenic Na^+/Ca^{2+} exchanger, producing an inward current that augments the rate of diastolic depolarization (DD), leading to an earlier occurrence of the subsequent action potential (AP), i.e. to an increase in the beating rate.

To test whether a concurrent voltage change, i.e. the DD, is actually required for the generation of CRDD, spontaneously beating single, SANC ($n = 9$) isolated from humanely killed rabbits were acutely voltage clamped (VC) at −60 mV (maximum diastolic potential) or −70 mV, and CRDD were imaged in the line scan mode using fluo-3 as Ca^{2+} indicator. CRDD, present during spontaneous beating, persisted during VC (Fig. 1). During the initial 400 ms of VC, a time corresponding to the next would-be AP if spontaneous firing were to have continued in the absence of VC, the total CRDD signal mass did not differ from that during DD during spontaneous beating (Fig. 1). With increasing time of VC, the total CRDD signal mass passed through a maximum (at 1.0 ± 0.2 s), then gradually decreased, and usually ceased at intervals > 5 s. We also observed that during VC the average level of cytosolic $[Ca^{2+}]$ gradually decreased to ~80 % of the level during spontaneous firing. When VC was removed, the cytosolic $[Ca^{2+}]$ and localized subsarcolemmal Ca^{2+} release returned to their pre-VC levels and spontaneous APs resumed. The addition of 50 μM Ni^{2+} to the bath prior to the voltage clamp did not affect the aforementioned results.

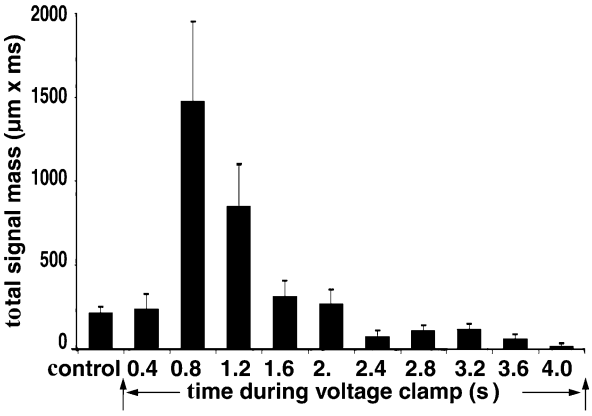

Figure 1. Total CRDD signal mass (means ± S.E.M., $n = 9$ cells) during DD during spontaneous beating (control) and during 'would-be' subsequent inter-AP intervals during voltage clamp. Each individual CRDD signal mass is estimated as FWHM × T_{50} × ½ F/F_0; FWHM, full width at half-maximum amplitude (F/F_0), where F and F_0 refer to peak and minimal fluorescence; T_{50}, the time above 50 % level of amplitude.

We conclude that the occurrence of localized RyR Ca^{2+} releases within a given DD during spontaneous beating does not require the concurrent membrane depolarization; its persistence, however, requires the regular occurrence of APs to provide Ca^{2+} influx sufficient to maintain cell and sarcoplasmic reticulum Ca^{2+} loading.

Bogdanov KY *et al.* (2001). *Circ Res* **88**, 1254–1258.

Huser J *et al.* (2000). *J Physiol* **524**, 415–422.

Rigg L & Terrar DA (1996). *Exp Physiol* **81**, 877–880.

All procedures accord with current National and local guidelines.

PC31

Inhibition of the basolateral Cl^- channel of rabbit gastric parietal cells by interleukin-1β is mediated by G_{12}/G_{13}-mediated Rho/Rho-kinase-dependent production of superoxide anion

T. Suzuki, Y. Ohira, A. Tanaka, M. Morii, H. Sakai and N. Takeguchi

Department of Pharmaceutical Physiology, Toyama Medical and Pharmaceutical University, Toyama 930–0194, Japan

Sub-pS Cl^- channels (0.3–0.4 pS) are present in the basolateral membrane of rabbit and rat parietal cells and have unique physiological roles. This Cl^- channel has a housekeeping role through dominating the cell membrane potential (Sakai *et al.* 1992), and the channel is activated via a prostaglandin E_2/nitric oxide/cyclic GMP-dependent pathway (Sakai *et al.* 1995). The channel activity is inhibited by pertussis toxin-insensitive G-protein-mediated production of superoxide anion (O_2^-) (Sakai

& Takeguchi, 1994). Recently, we found that interleukin-1β (IL-1β) inhibited the channel activity (Sakai *et al.* 2001).

Herein, we investigated whether IL-1β induces the intracellular production of oxygen radicals using the isolated rabbit gastric glands loaded with the oxidant-sensing fluorescent probe, dihydrofluorescein diacetate. We also studied the signalling mechanism of the IL-1β-induced production of O_2^-. Rabbits were killed by intraperitoneal administration of an overdose of urethane (> 2 g kg^{-1}). Preparation of gastric glands and whole-cell patch-clamp experiments were performed as previously described (Sakai & Takeguchi, 1994). Data are shown as means ± S.E.M. Fluorescence intensity is expressed in arbitrary units. Differences between groups were analysed by one-way ANOVA. Comparison between the two groups was made by Student's *t* test.

In the whole-cell recordings, the intracellular addition of superoxide dismutase (100 units ml^{-1}), a scavenger of O_2^-, and GDPβS (500 μM) abolished the IL-1β (1 ng ml^{-1})-induced inhibition of the Cl^- current. Northern blot analysis showed that $G_{\alpha 13}$ mRNA (5.8 and 7.9 kb) was highly expressed in rabbit gastric parietal cells. $G_{\alpha 12}$ mRNA (3.7 kb) was also expressed in the parietal cells. Y-27632 (10 μM), a specific inhibitor of Rho-kinase, abolished the IL-1β-induced effect. In dihydrofluorescein diacetate-loaded single parietal cells, IL-1β (1 ng ml^{-1}) increased the production of oxygen radicals. Recombinant IL-1 receptor antagonist (500 ng ml^{-1}) significantly inhibited the IL-1β-stimulated production of oxygen radicals (51.5 ± 5.5–9.3 ± 5.6 (arbitrary units), $P < 0.01$, $n = 4$). Y-27632 (10 μM) also inhibited the effect of IL-1β (53.0 ± 11.6–8.0 ± 3.1 (arbitrary units), $P < 0.05$, $n = 4$). We suggest that IL-1β inhibits the sub-pS Cl^- channels of rabbit gastric parietal cells by G_{12}/G_{13}-mediated Rho/Rho-kinase-dependent production of O_2^-.

Sakai H *et al.* (1992). *J Physiol* **448**, 293–306..

Sakai H & Takeguchi N (1994). *J Biol Chem* **269**, 23426–23430.

Sakai H *et al.* (1995). *J Biol Chem* **270**, 18781–18785.

Sakai H *et al.* (2001). *J Physiol* **533.P**, 15–16*P*.

All procedures accord with current local guidelines.

PC32

Oxidative stress and Ca^{2+} signalling in calf pulmonary artery endothelial cells

Jenny A. Wilkinson and Ron Jacob

Centre for Cardiovascular Biology & Medicine, King's College London, GKT School of Biomedical Sciences, London SE1 1UL, UK

We measured simultaneously cytosolic [Ca^{2+}] ([Ca^{2+}]$_i$) and oxidative stress (OS) in ATP-stimulated calf pulmonary artery endothelial cells (obtained from The European Collection of Cell Cultures), using fura-2 and the fluorescin-based probe C-H_2DCF, respectively. [Ca^{2+}]$_i$ is reported as the fura-2 340/380 nm fluorescence ratio and OS in arbitrary units of 495 nm fluorescence. Values quoted are means ± S.E.M. *P* values are for one-tailed, paired *t* tests or two-tailed, two-way ANOVA.

Stimulation with 100 μM ATP stimulated Ca^{2+} release with a peak [Ca^{2+}]$_i$ that was followed a few seconds later by a rapid increase in OS. In the continued presence of ATP, [Ca^{2+}]$_i$ fell to a maintained plateau, while the level of OS usually continued to rise slowly. After wash-out of ATP, 100 μM H_2O_2 caused a further increase in OS that was 9 ± 1 times larger than the response to ATP ($n = 25$ coverslips, 5 cultures). Pretreatment of cells with the anti-oxidant vitamin C (100 μM for 20–24 h) attenuated both the ATP- and H_2O_2-induced increases in OS (0.24 ± 0.01 to 0.12 ± 0.02, $P = 0.007$ and 3.0 ± 0.2 to 1.7 ± 0.2, $P < 0.001$, *t* test, $n = 3$ cultures, 40 coverslips) indicating that the C-DCF signal reflects OS.

Low concentrations of H_2O_2 can increase the IP_3 sensitivity of Ca^{2+} stores in permeabilised cells (Hu *et al.* 2000). Exposing cells to 5 μM H_2O_2 100 s prior to, and during a 10 min exposure to 100 μM ATP significantly enhanced the [Ca^{2+}]$_i$ peak from 3.38 ± 0.16 to 5.80 ± 0.53 ($n = 5$ cell cultures, $P < 0.001$, ANOVA). The [Ca^{2+}]$_i$ plateau was slightly but significantly increased. Both the initial increase in OS and that after 10 min ATP exposure were also significantly enhanced from 0.39 ± 0.09 to 0.61 ± 0.15 ($P < 0.001$) and from 0.65 ± 0.12 to 1.02 ± 0.19, respectively ($n = 5$ cell cultures, $P < 0.001$, ANOVA).

The potentiating effect of 5 μM H_2O_2 on the initial [Ca^{2+}]$_i$ peak was mimicked by raising [Ca^{2+}]$_o$ to 6 mM for 1 h prior to, and for the first 40 s of ATP exposure. This enhanced both the initial increase in OS (0.23 ± 0.06 to 0.61 ± 0.08; $P = 0.002$) and the level of OS observed after 10 min exposure to ATP (0.40 ± 0.08 to 0.64 ± 0.09; $P = 0.04$, unpaired, 1 culture, $n = 11$ coverslips), suggesting that the increased OS was a consequence of increased [Ca^{2+}]$_i$.

If the 5 μM H_2O_2 was removed before application of ATP the [Ca^{2+}]$_i$ peak was still potentiated (4.00 ± 0.33 to 6.84 ± 0.85; $n = 6$ cell cultures, $P < 0.001$, ANOVA). The effect on the OS was variable in different cell cultures, but overall was also significantly increased ($P < 0.001$, ANOVA).

There is potential for complex interactions between [Ca^{2+}]$_i$ and H_2O_2. Such interactions may shape physiological responses and also contribute to the endothelial dysfunction associated with many cardiovascular diseases, since oxidative stress is often observed in such conditions.

Hu Q *et al.* (2000). *J Biol Chem* **275**, 15749–15757.

This work was funded by Guy's and St Thomas' Charitable Foundation.

PC33

Elevated cytosolic calcium leads to remodelling of mitochondria and the endoplasmic reticulum

H. Llewelyn Roderick, Tony J. Collins, Michael J. Berridge and Martin D. Bootman

Laboratory for Molecular Signalling, The Babraham Institute, Babraham, Cambridge, UK

Cytosolic Ca^{2+} concentration is maintained at a level approximately 10 000-fold lower than that in the extracellular media, and is strictly regulated within defined limits by the interplay of Ca^{2+} channels, pumps and exchangers. The mitochondria and endoplasmic reticulum (ER) play a significant role in this process by storing and buffering Ca^{2+}. Ca^{2+} also regulates mitochondrial respiration, and is involved in protein synthesis and folding within the ER. Certain pathophysiological conditions, including apoptosis and neuronal excitotoxicity, have been ascribed to a sustained high intracellular Ca^{2+} concentration. In this study, we investigated whether the structure of intracellular organelles in HeLa cells is affected by prolonged increases in cytosolic Ca^{2+}. Application of a Ca^{2+} ionophore (ionomycin, 10 μM) to intact cells bathed in buffer containing 1.8 mM calcium resulted in the breakdown in the structure of mitochondria and the ER in 100 % of cells ($n = 110$ from 3 experiments). Confocal imaging of cells expressing ER- or mitochondrially targeted red/green fluorescent proteins (DsRed2 and EGFP) revealed that mitochondria initially swell, fragment

and then undergo permeability transition as determined by calcein release in response to elevated Ca^{2+}. Simultaneous with the fragmentation of mitochondria, the ER undergoes a dramatic vesicularisation followed by contraction towards the nucleus. In contrast, the Golgi and nuclear envelope were unaffected. The Ca^{2+}-induced breakdown of mitochondrial and ER membranes occurred in a concentration-dependent manner (EC_{50} ~30 μM) (10 cells per coverslip, 3 coverslips per calcium concentration from 1 to 1000 μM). In addition, the response was time dependent, in that a lower (~1 μM) Ca^{2+} concentration could cause organelle disruption if applied for periods greater that 30 min ($n = 20$ cells from 3 experiments). The effect was due to Ca^{2+} elevation rather than a non-specific consequence of ionomycin application, since the ionophore had no effect when extracellular Ca^{2+} was absent. Furthermore, the fragmentation of intracellular organelles could also be achieved by stimulation of heterologously expressed NMDA receptors (100 μM glutamate). The microtubule network was also fragmented by Ca^{2+} elevation. However, stabilisation of the microtubules with Taxol (10 μM for 30 min) failed to prevent organelle fragmentation. The fragmentation, however, was inhibited by application of Trolox (100 μM for 1 h), a lipid peroxidation inhibitor, or of MnTBaP (200 μM, 30 min), a superoxide dismutatase mimetic (3 coverslips from 3 experiments). This indicated that organelle fragmentation may occur as a result of lipid peroxidation occurring downstream of calcium elevation. Inhibition of calpains and caspases did not prevent the calcium-induced fragmentation. The disruption of organelles during elevated Ca^{2+} signals may contribute to the death of cells under pathological conditions, such as excessive NMDA receptor activity during neuronal excitotoxicity.

PC34

Spontaneous calcium oscillations control the development of metabotropic signalling in hippocampal neurons

Paul Cuddon, H. Llewelyn Roderick, Peter B. Simpson*, Michael J. Berridge and Martin D. Bootman

*Laboratory of Molecular Signalling, Babraham Institute, Cambridge and *Merck, Sharp and Dohme, Neuroscience Research Centre, Harlow, UK*

Despite the many studies regarding the development of the signalling components present in the plasma membrane of neurons, few have addressed the development of intracellular calcium signalling machinery. In this study, we investigated the effects of spontaneous calcium signals, resulting from synaptogenesis, on the maturation of metabotropic responses.

Post-natal (1–2 days old) Porton-Wistar rat pups were killed according to Home Office guidelines. Cultures of rat hippocampal neurons were prepared as described previously (Koizumi *et al.* 1999) and cells were studied between 4 and 21 days in culture. Functional synaptic networks were obtained by culturing neurons at 35 000 cm^{-2} ('high-density' neurons) and were compared against synaptically inactive neurons cultured at 5000 cm^{-2} ('low-density' neurons). Changes in intracellular calcium concentration were measured using video imaging of fura-2 (acetoxymethyl ester loading). Caffeine (40 mM) and carbachol (10 μM) were employed as agonists of ryanodine receptors and muscarinic acetylcholine receptors, respectively. All data are given as means ± S.E.M.

Responses to acute caffeine stimulation were absent in low-density neurons at any stage of the cultures. In contrast, high-density neurons began to show calcium release in response to caffeine following 9 days in culture. These caffeine-evoked calcium signals progressively increased in amplitude from day 9 to 21, reaching a peak amplitude of 286 ± 34 nM ($n = 33$ cells). Similar results were obtained using carbachol: low-density neurons did not respond to carbachol at any stage, whereas high-density neurons responded to carbachol from day 9. The amplitude of the carbachol responses peaked at 264 ± 60 nM ($n = 26$ cells) on day 15.

Superfusion with 25 mM KCl depolarised the neurons, giving calcium signals that served to increase the loading of the intracellular calcium stores. Such store loading allowed similar amplitude caffeine-evoked calcium signals in low- and high-density neuronal cultures. KCl application also promoted the response of low-density neurons to carbachol. However, there was a significant difference in the amplitude of the carbachol-evoked calcium signals between low- and high-density neurons. This indicates that the development of metabotropic signalling, but not ryanodine receptor expression, was dependent on neuronal density.

The development of caffeine- and carbachol-evoked responses from day 9 onwards in the high-density neurons correlated with the onset of spontaneous calcium oscillations, most probably arising from the formation of synaptic contacts between cells. Such oscillations were rare in the low-density neuronal cultures. The spontaneous activity serves a dual purpose of increasing the loading of intracellular calcium stores and also promoting the expression of proteins involved in metabotropic responses.

Koizumi S *et al.* (1999). *Neuron* **22**, 125–137.

All procedures accord with current UK legislation.

PC35

Spatio-temporal aspects of damage-induced proliferation in chick vestibular epithelial cultures

J.E. Bird and J.E. Gale

Department of Physiology, University College London, Gower Street, London WC1E 6BT, UK

In the damaged avian inner ear regeneration occurs when supporting cells are triggered to proliferate after the loss of nearby hair cells. In order to study the signalling events that regulate and stimulate the activation of proliferation in hair cell epithelia we have adapted an epithelial culture preparation using thermolysin-treated utricular epithelia. Embryonic day 21 pre-hatch chicks were killed humanely and the utricles isolated. Utricles were treated with thermolysin for 45 min, facilitating the removal of the epithelial sheet from the underlying basement membrane for subsequent culture (Warchol, 2002). A nitrogen laser based ablation system (Micropoint™, Photonic Instruments, USA) attached to the epifluorescence port of the microscope allowed precise control of the timing and magnitude of the epithelial damage. 5-Bromo-2′-deoxyuridine (BrdU), which is incorporated into the DNA of cells during s-phase, was used to assess the induction of proliferative activity. Epithelia were subjected to a 2 h pulse of BrdU (3 μg ml^{-1}) prior to fixation and labelled using BrdU antibodies. BrdU pulses were applied between 6 and 24 h after laser ablation. A minimum of four epithelia was used for each time-point. BrdU-positive nuclei were counted within a 120 μm radius circle centred over the ablation site. The number of s-phase cells varied appreciably over the 6–26 h period analysed. Two temporally distinct increases of 301 ± 72 % ($n = 4$) and 438 ± 153 % ($n = 6$, mean ± S.E.M.) over control levels were seen at 12 and 24 h, respectively. In addition to investigating the temporal distribution of s-phase entry, we

were able to bin BrdU-positive cells spatially using co-ordinate data calculated with Metamorph imaging software (UIC, USA). We used concentric circles of radius 60 and 120 μm to form two binning regions (inner and outer) of 0–60 and 60–120 μm. S-phase entry in the outer region was elevated by 295 ± 218 % ($n = 4$) and 330 ± 120 % ($n = 6$) over control levels at 12 and 24 h, respectively. In the inner region s-phase entry was not significantly elevated over controls at 12 h, but was seen to markedly increase after 24 h by 1323 ± 504 % ($n = 6$) over controls.

The temporal data suggest that laser ablation triggers two waves of s-phase entry occurring 12 and 24 h after damage. In cells proximal to the lesion site s-phase entry is delayed when compared with more distal cells. We tentatively suggest that at early time points the primary function of cells surrounding the lesion is repair of the wound, and it is this activity which delays s-phase entry in those cells.

Warchol ME (2002). *J Neurosci* **22**, 2607–2616.

This work was supported by The Wellcome Trust, The Royal Society and a Medical Research Council Studentship to J.E.B.

All procedures accord with current UK legislation.

PC36

Inhibition of inositol 1,4,5-trisphosphate ($InsP_3$)-induced calcium release by neuronal calcium binding proteins (CaBP)

H. Llewelyn Roderick*, Martin D. Bootman*, Humbert De Smedt†, Jan B. Parys†, Ludwig Missiaen† and Nael N. Kasri†

**Laboratory of Molecular Signalling, Babraham Institute, Cambridge CB2 4AT, UK and* †*Laboratorium voor Fysiologie, K.U. Leuven, Leuven, Belgium*

It has recently been demonstrated that CaBP interacts with and activates $InsP_3Rs$, providing a novel mechanism for calcium release independent of $InsP_3$ production (Yang *et al.* 2002). Using a combination of calcium imaging, calcium flux studies and biochemical approaches, we have investigated the role of CaBPs in regulating $InsP_3Rs$.

Glutathione *S*-transferase (GST) pull-down experiments using GST-tagged NH_2-terminal regions of $InsP_3Rs$ as bait and purified CaBP as prey in the presence of 200 μM calcium concentration revealed that CaBP interacted with a region of the type 1 $InsP_3R$ encompassing amino acids 1–224. Peptide mapping of the site of interaction revealed that CaBPs interacted with a region encompassing amino acids proline 49 to asparagine 81, which corresponded to the calcium-independent calmodulin binding region. Furthermore, unlike the previously reported findings (Yang *et al.* 2002), we demonstrate that this interaction occurs completely independently of calcium. Imaging of fura-2-loaded COS-7 cells overexpressing GFP-tagged CaBPs revealed that CaBP could inhibit calcium release from internal stores in response to an $InsP_3$-generating agonist (ATP; 0.5 to 100 μM). Data are expressed as means ± S.E.M. and were analysed for significance using a Student's *t* test. With 0.5 μM ATP, the integrated calcium response was significantly reduced from 12 618 ± 1879 nM s ($n = 27$ cells) in control cells to 4921 ± 1839 nM s ($n = 4$ cells) in CaBP-expressing cells ($P < 0.05$). With 1 μM ATP, the integrated calcium response was decreased from 24 187 ± 1861 nM s in control cells ($n = 32$ cells) to 9655 ± 1757 nM s ($n = 13$) in CaBP-expressing cells ($P < 0.05$). In addition to decreasing the magnitude of ATP-evoked calcium signals, CaBP expression reduced the proportion of responding cells. With 0.5 μM ATP, 73 % of control cells ($n = 44$) and 18 % of CaBP-expressing cells ($n = 22$) responded. The calcium release in response to a supramaximal ATP concentration (100 μM) was not significantly different between control and CaBP-expressing cells, indicating that the intracellular calcium stores were not compromised by CaBP expression. To directly test the effect of CaBPs on $InsP_3$-induced calcium release we performed $^{45}Ca^{2+}$ flux experiments using saponin-permeabilised A7r5 cells. In the presence of 100 nM cytosolic calcium, 1 μM $InsP_3$ released 30 % of the total calcium store. CaBP, however, did not release calcium from internal stores. In conclusion, CaBPs do not appear to act as endogenous activators for $InsP_3Rs$. Rather they inhibit $InsP_3$-mediated calcium release.

Yang J *et al.* (2002). *Proc Natl Acad Sci* **99**, 7711–7716.

PC37

Effects of endothelin-1 and inositol 1,4,5-trisphosphate on calcium signalling in rat ventricular and atrial myocytes

Lauren Mackenzie, Martin D. Bootman, Michael J. Berridge and Andrew P. Proven

The Babraham Institute, Babraham, Cambridge CB2 4AT, UK

Endothelin-1 (ET-1) acts via multiple signalling pathways to modulate the inotropic status of the heart and can cause arryhthmias. This study compared the effects of ET-1 on the patterns and kinetics of calcium signalling in atrial and ventricular myocytes, and examined the role of $InsP_3$ in changes evoked by ET-1.

Myocytes were enzymatically isolated from rats killed by cervical dislocation in accordance with Schedule 1 Home Office regulations. Cells were electrically paced at 0.3 Hz and calcium changes were monitored using indo-1. Experiments were conducted at room temperature. All statistics represent means ± S.E.M.

In response to 100 nM ET-1, atrial myocytes displayed a brief (~3 min) phase of negative inotropy followed by a positive inotropic response that peaked at 254 ± 17 % relative to control amplitude responses ($n = 7$ cells) after 16 min exposure. In contrast, ventricular myocytes exhibited no negative inotropic phase, and achieved a maximum inotropic response of 193 ± 22 % after 21 min ($n = 15$ cells). ET-1 stimulation caused substantial numbers of spontaneous calcium transients (SCTs) in atrial and ventricular cells. These events were rare in control recordings. For atrial cells, SCTs began at the onset of the positive inotropic response, after 5 min of ET-1 simulation. They progressively increased in frequency and amplitude such that at 25 min of ET-1 stimulation an average of 19 ± 1.4 SCTs per 30 s sample period ($n = 7$ cells). For ventricular myocytes, SCTs arose within 1 min of ET-1 stimulation and reached a maximum of 12 ± 2.2 SCTs ($n = 15$ cells).

Stimulation with a membrane-permeant form of $InsP_3$ ($InsP_3$ ester; 10 μM) caused a modest positive inotropic response in both atrial and ventricular myocytes. The most prominent effect of the $InsP_3$ ester was to provoke the occurrence of SCTs. Consistent with the greater $InsP_3$ receptor expression in atrial myocytes, the $InsP_3$ ester-evoked SCTs were more frequent in the atrial cells (25 ± 7.5 events per 30 s sample period; $n = 4$ cells) than in ventricular cells (6 ± 2 events per 30 s sample period; $n = 14$ cells). In both cell types, the ET-1 and $InsP_3$ ester-evoked SCTs were inhibited by 2-aminoethoxydiphenyl borate (2 μM). These data indicate subtly different effects of ET-1 on calcium

signalling in atrial and ventricular cells. Furthermore, $InsP_3$ may underlie some of the pro-arrythmogenic actions of ET-1, but does not significantly influence the inotropic status of these cells.

All procedures accord with current UK legislation.

PC38

Arachidonic acid-evoked non-capacitative calcium entry is dominant over capacitative calcium entry

Anthony M. Holmes*, H. Llewelyn Roderick*, Michael J. Berridge*, Fraser McDonald† and Martin D. Bootman*

**Laboratory of Molecular Signalling, The Babraham Institute, Cambridge CB2 4AT and †Bone Research Unit, Department of Orthodontics and Paediatric Dentistry, Floor 22, Guy's Tower, UMDS, London SE1 9RT, UK*

In many cell types, depletion of intracellular calcium stores promotes the opening of plasma membrane channels resulting in capacitative calcium entry (CCE). There is growing evidence for non-capacitative calcium entry (NCCE) pathways activated by lipid messengers including arachidonic acid (AA). CCE and NCCE cannot be simultaneously activated (Luo *et al.* 2001; Mignen *et al.* 2001; Moneer & Taylor, 2002), although it is not clear how this mutual antagonism is achieved.

Calcium signals were monitored in fura-2-loaded HEK-293 and Saos-2 cells. All experiments were performed at room temperature (~20 °C). AA (30 μM) and the calcium-ATPase inhibitor thapsigargin (2 μM) were applied exogenously to activate NCCE and CCE, respectively.

With both HEK-293 and Saos-2 cells, thapsigargin and AA generated biphasic responses resulting from mobilization of a common intracellular calcium store followed by a prolonged calcium influx phase. Despite mobilization of a common calcium pool, these agents did not activate the same calcium influx pathway. Thapsigargin activated a classical CCE pathway that was inhibited by 2-aminoethoxydiphenyl borate (2-APB; 100 μM) (HEK-293, $n = 20$ cells; Saos-2, $n = 12$ cells) and gadolinium (Gd^{3+}; 1 μM) (HEK-293, $n = 20$ cells; Saos-2, $n = 14$). The calcium influx activated by AA was not affected by 2-APB or Gd^{3+}, but was blocked by LOE-908, a diagnostic for NCCE (Moneer & Taylor, 2002) (HEK-293, $n = 12$ cells; Saos-2, $n = 14$ cells).

Stimulation of cells with thapsigargin in the presence of Gd^{3+} produces a transient response reflecting only the mobilization of intracellular stores. Subsequent addition of AA does not cause any further change in calcium, indicating that under these conditions NCCE was not activatable. Similar observations have been suggested to indicate that activation of CCE is solely sufficient to prevent NCCE (Luo *et al.* 2001). However, addition of AA to cells during an ongoing CCE signal (i.e. no Gd^{3+} present) caused a rapid and transient decline of the intracellular calcium concentration, followed by a progressive increase in calcium that was fully inhibited by LOE-908 (HEK-293, $n = 20$ cells; Saos-2, $n = 13$ cells). This pattern of response essentially represented the switch from CCE to NCCE. In our hands, AA appears to be a dominant signal for calcium influx over CCE – it rapidly inhibits ongoing CCE and steadily promotes NCCE. The presence of Gd^{3+} during CCE activation may cause sequestration of channel subunits also required for NCCE, therefore inhibiting subsequent AA responses.

Luo D *et al.* (2001). *J Biol Chem* **276**, 20186–20189.

Mignen O *et al.* (2001). *J Biol Chem* **276**, 35676–35683.

Moneer Z & Taylor C (2002). *Biochem J* **362**, 13–21.